Reprinted from

BRACHYTHERAPY

An International Multidisciplinary Journal

Official Journal of the American Brachytherapy Society

VOLUME 1, NUMBER 2, 2002

Measurements of the dosimetric constants for a new ^{103}Pd brachytherapy source

Stephen W. Peterson, Bruce Thomadsen

ELSEVIER

Brachytherapy 1 (2002) 110–119

BRACHYTHERAPY

Measurements of the dosimetric constants for a new ^{103}Pd brachytherapy source

Stephen W. Peterson[1], Bruce Thomadsen[1,*]

[1]*Department of Medical Physics, University of Wisconsin–Madison, 1300 University Avenue, Madison, WI 53706, USA*

Abstract

Purpose: This report provides dosimetry information for a new brachytherapy ^{103}Pd source (Model 2335) manufactured by Best Medical International and, through comparisons with data from another published report for the same source, presents a suggested hybrid dataset for clinical applications.

Methods and Materials: Dose measurements were made using thermoluminescent dosimeters (TLD), with the ^{103}Pd source in the center of a Virtual Water phantom on a rotating insert, allowing for a number of different possible angles, and 12 TLD cubes (1.0 × 1.0 × 1.0 mm) and 16 TLD rods (1.0 × 1.0 × 3.0 mm) arranged in an outward spiral pattern at distances ranging from 0.5 to 5.0 cm. All measurements are based on the 2000 correction of the National Institute of Standards and Technology 1999 standard.

Results: From these measurements, tables are presented for the radial dose function and the anisotropy function. The dose rate constant = 0.71 ± 0.07 cGy h^{-1} U^{-1} and the anisotropy constant = 0.96 ± 0.03.

Conclusions: The dose rate constant for the hybrid = 0.70 and the anisotropy constant for the hybrid = 0.92, Hybrid tables are presented.

Keywords: ^{103}Pd; Brachytherapy; Dose rate constant; Anisotropy function; Radiotherapy dosimetry

Introduction

Permanent brachytherapy implants often use ^{103}Pd and ^{125}I. The dosimetric characteristics of each new source must be measured experimentally before it can be used in the clinic (1). This article presents dosimetric information for a new brachytherapy ^{103}Pd source manufactured by Best Medical International (Springfield, VA), as described by Task Group 43 (TG-43) of the American Association of Physicists in Medicine (AAPM) (2), and combines the results with another data set determined for the same source model, making suggestions for factors to be used clinically. All values in this article are traceable to the National Institute of Standards and Technology (NIST) 1999 S_K standard, as revised on September 2, 2000.

Methods and materials

The measurements were made in a water equivalent phantom with a centrally located source surrounded by thermoluminescent dosimeters (TLDs) in a spiral pattern.

^{103}Pd source

The Best Model 2335 ^{103}Pd radioactive source has outside dimensions of 5 mm in length and 0.8 mm in diameter. Figure 1 shows the schematic of the source. The 5-mm length, when combined with 5-mm spacers in preloaded needles, places the centers of all sources in planes corresponding to standard 5-mm ultrasound cut spacing, regardless of the combination of sources and spacers. The source jacket consists of a double titanium wall, 0.035 mm thick, with one end closed and the other end laser welded. The inside of the source consists of six resin beads containing ^{103}Pd, with each bead having a diameter of 0.56 mm, with three beads on each end of the source separated by a tungsten marker 1.19 mm in length. Palladium-103 has a half-life of 16.99 days and decays through electron capture to a metastable state of ^{103}Rh. Most of the radiation comes from fluorescence after de-excitation of the ^{103m}Rh to the ground state in the form of characteristic X-rays, with energies of 20.07 keV (23.1%), 20.22 keV (43.8%), and 22.72 keV (11.8%) (3). The decay includes some low-yield gamma rays with higher energies, but the frequencies are generally of the order of 0.01%.

The low-energy photons emitted by the ^{103}Pd source suffer severe attenuation in water, as well as in the phantom material used for this experiment (described below), with

Received 21 March 2002; received in revised form 15 May 2002; accepted 16 May 2002.

* Corresponding author. Department of Medical Physics, 1300 University Avenue, Room 1530, Madison, WI 53706.

1538-4721/02/$ – see front matter
PII: S1538-4721(02)00015-6

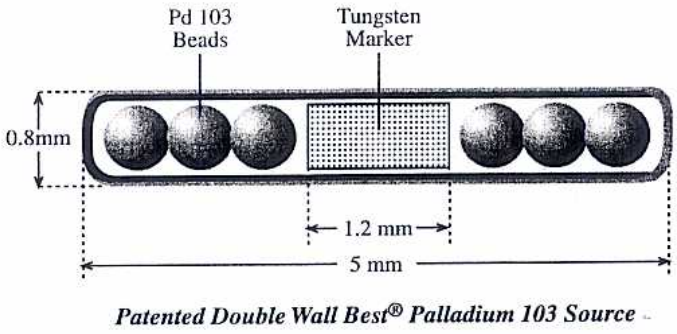

Fig. 1. Schematic of the Best ^{103}Pd source (courtesy of Best Medical International).

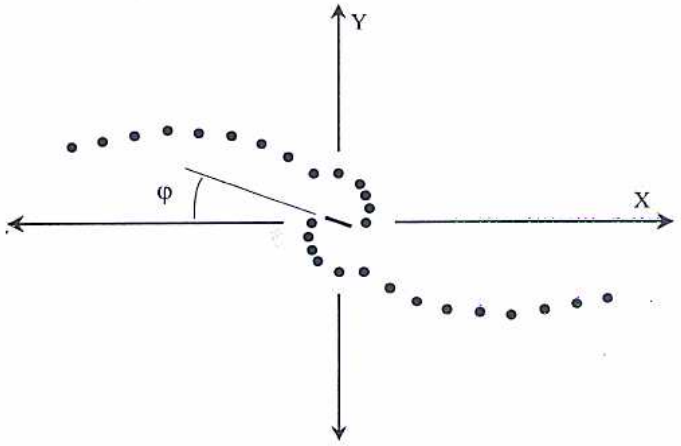

Fig. 2. Layout of the holes in each Virtual Water phantom.

only approximately 0.25% of the signal at 1 cm reaching the farthest measurement point 5 cm distant from the source (on the basis of absorption and a $1/r^2$ relationship). This attenuation necessitated very long exposure times to obtain reliable measurements. The long exposure time for each run, combined with the short half-life of the radionuclide and the limited number of data points in each run, meant that this experiment required a large number of sources to complete. As a result, 23 radioactive sources were used during the measurement process. These sources contributed to 34 independent experiments: 10 focused on calculating the dose rate constant and the radial dose function, and 24 focused on determining the anisotropy function. Each independent run incorporated 28 TLDs—2 for each data point.

The sources used in the work were assayed in a well-type ionization chamber (CNMC Company Inc., Nashville, TN) that had been calibrated against NIST-calibrated sources of this same type. The calibration of the sources followed the 1999 standard ($S_{K,N99}$) from NIST as corrected in 2000 for the wide-angle free-air chamber measurement errors that occurred in 1999. The air kerma strength measurements for each source were generally approximately 1.4 U, with the source strengths never varying by more than 0.7 U.

Virtual Water phantoms

All dose-distribution measurements were made in phantoms constructed from Virtual Water (MED-CAL, Inc., Verona, WI). Six phantoms were formed from pairs of 15.2 × 15.2 × 5.0 cm blocks. One half of each phantom pair contained 28 holes to hold TLDs, as shown in Fig. 2; the holes were arranged to form a spiral-type pattern to ensure that all of the holes were within the line of sight of the radioactive source. The blocks carried two holes at each of the given distances: 0.5, 0.6, 0.7, 0.8, 0.9, 1.0, 1.5, 2.0, 2.5, 3.0, 3.5, 4.0, 4.5, and 5.0 cm. The holes were customized for the size of the TLD at the location and were set such that the center of the TLD fell in the plane parallel to the surface and containing the center of the source. The center of the pattern contained a cylindrically shaped Virtual Water plug to hold the ^{103}Pd source. Two plugs were used: one held the source vertically, to allow measurements at all distances in the plane of the source's perpendicular bisector; the other oriented the source axis in the plane of the TLD. With the latter orientation, the angle of the axis could be rotated to place the ^{103}Pd source at any arbitrary angle with respect to the TLDs.

The calculated dose rate to the TLDs in Virtual Water requires a conversion to the dose rate in water. For this conversion, factors from Williamson, as shown in Table 1, were used (J. Williamson, personal communication, 2001). Although the conversion factors were calculated for Solid Water (RMI-Gammex, Middleton, WI), the chemical formulas for the two are essentially identical. Dosimetric factors determined for Solid Water can be used with Virtual Water.

Thermoluminescent dosimeters

All of the dose measurements were made with LiF TLD-100 TLDs (Bicron Corp., Solon, OH). The use of two different sizes of TLD allowed a compromise between the size of the detector (and, therefore, the geometric uncertainty of the measurement location) and the size of the reading (and, thereby, the associated uncertainty). Measurements 1 cm and closer to the source were recorded with 1.0 × 1.0 × 1.0 mm cubes, whereas at distances greater than 1 cm, measurements were taken with 1.0 × 1.0 × 3.0 mm rods.

Table 1
Factors to convert readings taken in Solid Water to project the response in water for LiF exposed to ^{103}Pd radiation

Distance (cm)	Conversion factor
0.5	1.024
0.6	1.030
0.7	1.033
0.8	1.037
0.9	1.042
1.0	1.047
1.5	1.078
2.0	1.093
2.5	1.136
3.0	1.152
3.5	1.181
4.0	1.211
4.5	1.234
5.0	1.259

The TLD calibration consisted of an annealing cycle for the TLDs, heating them to 400°C for 1 h and then to 80°C for 24 h. Calibration of the sources used exposures between 0.1 and 0.2 Gy of ^{60}Co radiation. The TLDs were read at least 24 h later by using, initially, a Harshaw Model 2000D TL detector with a Model 2080 TL analyzer (Bicron Corp.), but in later experiments, by using a Harshaw TLD reader 5500 (Bicron Corp.). After readout, the TLDs were returned to the 80°C oven for another 24 h before subsequent use. This process was repeated three times to ensure the stability of the TLD readings. Individual calibration factors (the dose delivered to the dosimeter divided by the charge reading based on the last set of readings) were used to convert subsequent charge readings into doses in the experimental measurements. After being used in an experiment, the TLDs were reannealed and recalibrated for the next set of readings.

The TLDs were then loaded into the phantoms, and the radioactive source was placed in position and left in place for times calculated to deliver between 1 and 3 Gy to the dosimeters. The dosimeters were removed at different times to keep their doses within this range. The exposure time of the TLDs ranged from 6 to 21 days, depending on the initial source strength and distance from the source. The TLDs were then read, by using the same procedure as used for calibration. These readings were used to calculate the dose rate to water at the TLD position per unit source strength ($\dot{D}/S_K$), by using the formula

$$\left(\frac{{}_{m}\dot{D}(r,\theta)}{{}_{eff}S_k}\right)_{Water} = \frac{R \cdot CF \cdot W}{1.41 \cdot S_k \cdot t_{eq}}, \quad (1)$$

where ${}_{m}\dot{D}(r,\theta)$ is the dose rate measured at the point (r,θ), R is the reading from the TLD, corrected for background (cGy/nC), CF is the calibration factor for the individual TLD (nC), W is the Solid Water to water conversion factor (Table 1), S_K is the source strength at the start of measurement (μGy·m^{-2}·h^{-1}; U), and t_{eq} is the time equivalent to account for the decay of the source strength during the measurements:

$$t_{eq} = (1 - e^{[-\ln 2 \cdot t/t_{1/2}]}) \cdot t_{1/2}/\ln 2 \quad (2)$$

The correction for the energy response of LiF between ^{60}Co and ^{103}Pd was 1.41. Hartmann *et al.* (4) reported a value for this factor of 1.40% ± 2.8%. Weaver (5) calculated the energy response to be 1.39 ± 0.03 for dose to water. Meigooni *et al.* (6) determined the correction due to the energy difference to be 1.41% ± 3%. The energy response correction factor (1.41) was used to be consistent with previous reports.

Dose equations

All of the data calculations followed the formalism set up in the report of TG-43 of the AAPM. The basic equation for the dose at a point is

$$\dot{D}(r,\theta) = S_K \Lambda [G(r,\theta)/G(r_o,\theta_o)] g(r) F(r,\theta), \quad (3)$$

where $\dot{D}(r,\theta)$ is the dose rate at point (r,θ), S_K is the air kerma strength of the source, Λ is the dose rate constant, $G(r,\theta)$ is the geometry factor, $g(r)$ is the radial dose function, $F(r,\theta)$ is the anisotropy function, r_0 = 1 cm, and θ_0 = 90°. For a discussion of these quantities, the reader should refer to the AAPM report (2).

The dose rate constant, Λ, is defined as the dose rate to water at a distance of 1 cm on the transverse plane from a unit air-kerma-strength source in a water phantom. Measurements for the dose rate constant and the radial dose function were taken in the Virtual Water phantoms by using the insert that holds the source vertically, as described previously. The equation for the dose rate constant is

$$\Lambda = \left[\frac{\dot{D}(r_0,\theta_0)}{S_K}\right]_{Water} \quad (4)$$

The radial dose function, $g(r)$, accounts for the absorption and scatter in the medium along the transverse axis of the source. Measurements for $g(r)$ used the same setup as that to determine the dose rate constant, with values from

$$g(r) = \dot{D}(r,\theta_0) G(r_0,\theta_0) / \dot{D}(r_0,\theta_0) G(r,\theta_0) \quad (5)$$

The derivation of the dosimetric quantities used three forms of the geometry factor, for reasons considered in "Discussion." The first part of this article considers the activity of the source to be uniformly distributed over the length occupied by the active spheres (0.455 cm), as shown in Fig. 1. The equation for $G(r,\theta)$ for the line source becomes

$$G(r,\theta) = \frac{\tan^{-1}\left(\frac{r\cos(\theta) + L_A/2}{r\sin(\theta)}\right) - \tan^{-1}\left(\frac{r\cos(\theta) - L_A/2}{r\sin(\theta)}\right)}{L_A r \sin(\theta)}, \quad (6)$$

where L_A is the active length of the source. On the perpendicular bisector, the equation degenerates to

$$G(r,\pi/2) = \frac{2\tan^{-1}(L_A/2r)}{L_A r} \quad (7)$$

and on the source axis to

$$G(r,\theta^0) = \frac{1}{L_A}\left(\frac{1}{r - L_A/2} - \frac{1}{r + L_A/2}\right) \quad (8)$$

The second approach to the geometry factor models each of the six active spheres within the source as point sources. The formula for the geometry factor for the complete source becomes

$$G(r,\theta) = \frac{1}{6}\left(\sum_{n=1}^{6} \frac{1}{r^2 + 2rr_n\cos(\theta) + r_n^2}\right), \quad (9)$$

where r_n is the distance of each source sphere to the center of the linear source, with distances r_{1-3} being positive and r_{4-6} being negative. The equation on the perpendicular bisector is

$$G(r,\pi/2) = \frac{1}{6}\left(\sum_{n=1}^{6}\frac{1}{r^2 + r_n^2}\right), \quad (10)$$

and along the source axis the factor becomes

$$G(r,0^0) = \frac{1}{6}\left(\sum_{n=1}^{6}\frac{1}{r^2 + 2rr_n + r_n^2}\right) \quad (11)$$

Finally, the source as a whole is modeled as a single point source, and the geometry factor becomes

$$G(r) = \frac{1}{r^2}. \quad (12)$$

The anisotropy function, $F(r,\vartheta)$, accounts for the remaining anisotropy of the dose distribution around the source. Measurements were taken, by using the setup previously described, with the Virtual Water plug that allowed the ^{103}Pd source to lie in the plane of the TLDs. A total of 24 experimental runs were performed, with the source being set to various angles. The range of source angles used during these measurements, as shown in Fig. 2, was from 0° to 165°. The equation for the anisotropy function is

$$F(r,\theta) = \dot{D}(r,\theta)G(r,\theta_0)/\dot{D}(r,\theta_0)G(r,\theta) \quad (13)$$

The anisotropy factor, $\phi_{an}(r)$, is the ratio of the dose rate at distance r, averaged with respect to the solid angle, to the dose rate on the transverse axis at the same distance, defined as

$$\phi_{an}(r) = \quad (14)$$

$$\frac{\int_0^{\pi}\dot{D}(r,\theta)\sin\theta d\theta}{2\,\dot{D}(r,\theta_0)} = \frac{\int_0^{\pi}F(r,\theta)G(r,\theta)\sin\theta d\theta}{2G(r,\theta_0)}$$

The anisotropy constant, ϕ_{an}, a correction for anisotropy, independent of distance, is used for groups of sources when the exact angle of each is not known:

$$\bar{\phi}_{an} = \frac{\int_0^{5cm} g(r)\phi_{an}(r)dr}{\int_0^{5cm} g(r)dr} \quad (15)$$

Results

Uncertainty

The values used in our uncertainty calculations are listed in Table 2. The error determined by statistical methods is the Type A error. The 10% value is the standard deviation of the 10 measurement values for the dose rate constant. Type B error is based on measurements and experimental uncertainty values. By using these values, the uncertainties were calculated for the constants and other factors with standard error propagation equations. Measurements of the source strength, performed at the Accredited Dosimetry Calibration Laboratory at the University of Wisconsin–Madison, had an uncertainty of 2%, with 1.5% contributed from the NIST calibration. The TLD calibration factors had an uncertainty of 3%, and the uncertainty in the distance between the TLDs and the source varied from approximately 4.5% at 0.5 cm to approximately 0.45% at 5.0 cm. The total calculated uncertainty for the dose rate constant was 11.7%. The uncertainty calculated on the anisotropy constant was 3.4%. The uncertainty is also shown on some figures as error bars.

Dose rate constant

Evaluation of the dose rate constant used the results of 10 runs. The results were averaged, and the dose rate constant, Λ, was found to be 0.71 ± 0.07 cGy·h^{-1}·U^{-1}, as shown in Table 3.

Radial dose function

The radial dose function, $g(r)$, was calculated from the measurements taken between 0.5 and 5 cm. These results, from four independent runs, were combined and averaged to obtain the radial dose function. The values from these measurements are recorded in Table 4 and shown graphically in Fig. 3. The data were fitted to a fifth-order polynomial by following the form used in TG-43:

$$g(r) = a_0 + a_1 r + a_2 r^2 + a_3 r^3 + a_4 r^4 + a_5 r^5, \quad (16)$$

where $a_0 = 1.6917$, $a_1 = -0.8391$, $a_2 = 1.3190 \times 10^{-1}$, $a_3 = 9.3691 \times 10^{-3}$, $a_4 = 5.2798 \times 10^{-3}$, and $a_5 = 4.5695 \times 10^{-4}$, with an R^2 value of 0.9997. The polynomial turns up and rapidly increases outside the range of experimental data and so should not be used beyond 5 cm. An exponential fit more likely closely follows the physical functionality of the quantity. The modeled equation is $g(r) = \alpha e^{-\beta r}$, with coefficients of $\alpha = 1.7830$ and $\beta = 0.5966$ and an R^2 value of 0.9997. Another option, which would eliminate the difficulties associated with the polynomial, is to use a fitting function to model the radial dose function (7).

Anisotropy function

The anisotropy function, $F(r,\theta)$, was determined by a series of independent measurements taken over 22 different source angles. As shown in Fig. 2, the TLD dose measurements were not taken at regular 10° intervals, but over a diverse range of angles from 0° to 90°. A total of 24 different data points were condensed into the normal 10° increment values by weighting the values and then averaging them. Typically, four or five data points were used in determining the value for each angle, but the number varied. The values were weighted inversely by the difference between the data point angle and the tabular angle. This process reduces the experimental uncertainty for the specified point by increas-

Table 2
Uncertainty calculations for the experimental determination of the dose rate constant

Source of uncertainty	Type A (%)	Type B (%)
Standard deviation of Λ	10.0	
Source strength measurement		2.0
TLD dose calibration		3.0
TLD readings 1		3.0
TLD readings 2		3.0
Distance between source and TLD		2.3
Each type combined in quadrature	10.0	6.0
Combined standard uncertainty	11.7	

TLD = thermoluminescent dosimeter.

ing the data used in its determination. These data were further modified by smoothing the curves on graphs as functions of distance for a given angle and angle as a function of distance. The resulting graphs are shown in Fig. 4, and the values for selected distances and angles are listed in Table 5, where the anisotropy factors are also listed.

Anisotropy constant

The value for the anisotropy constant depends on the selection of anisotropy function values over which the integration is performed. Restricting the integration to integral values of r (as in the TG-43 report) yields an anisotropy constant of 0.96 ± 0.03, whereas, in this case, including the half-centimeter and the subcentimeter entries also produces a value of 0.96 ± 0.02.

Discussion

Geometry factors

Each of the three formats used for the geometry factors finds an application. The model with each source sphere approximated as a point source is indistinguishable from a more rigorous model at the range of distances considered in this work. However, in clinical practice, the user likely will simplify the model and assume that the active length runs from the extreme limits of the spheres (ignoring the inactive marker in the center). Deriving the factors for users applying the geometry factors for the simpler model will result in correct calculated doses. In cases where individual source orientation is not considered (most of the current applications), the point source model becomes appropriate, and the geometry factor approximated by an inverse square relationship should be used in determining the other functions. The difference between the six point sources model and the line source model can only really be seen at close distances (closer than 2 cm). Table 6 shows the percentage difference between the two geometry factors.

Dose rate constant comparison

Table 3 compares the value for the dose rate constant with that determined by Meigooni *et al.* (8) for this source model and the dose rate constant determined for other ^{103}Pd sources (2, 9, 10). From the values given for the dose rate constant of the Best ^{103}Pd source, the suggested value for clinical use would be 0.7. The three values for the dose rate constant were averaged, weighting the result heavily toward this work because of the differences in phantom material used by Meigooni, as discussed below.

Radial dose function comparison

Figure 3 shows the radial dose function, the raw data with error bars, and the polynomial fit. Also shown is the radial dose function calculated in this work as compared with the data from TG-43 (2), experimental data from Meigooni *et al.* (8) and other ^{103}Pd sources. Although they are extremely close, there is a shift (for the same source model) between the measurements by Meigooni and those in this report. Samples of the Solid Water phantom material used by

Table 3
Comparison between some of the dosimetric constants for the Best and Theragenics ^{103}Pd sources

Source	Method	Dose rate constant ($cGy \cdot h^{-1} \cdot U^{-1}$)	Anisotropy constant			
			Weighted		Simple average	Method unspecified
			$g(r)$	$g(r)/r^2$		
Best (this work)	TLD	0.71	0.96	0.96	0.94	
Best (8)	TLD	0.69			0.89	
	MC	0.67			0.88	
Hybrid	TLD, MC	0.70	0.92			
Theraseed (2)	TLD	0.68				0.90
MED3633 (9)	TLD	0.68				0.95
Intersource (10)	TLD	0.70			0.90	
	MC	0.70			0.90	

TLD = thermoluminescent dosimeter; MC = Monte Carlo.

Table 4
Measured radial dose function values for Best ^{103}Pd source

Distance (cm)	Radial dose function		
	Six spheres	Line source	Point source
0.5	1.328	1.307	1.248
0.6	1.257	1.245	1.211
0.7	1.165	1.159	1.140
0.8	1.101	1.098	1.088
0.9	1.052	1.050	1.046
1.0	1.000	1.000	1.000
1.5	0.740	0.742	0.749
2.0	0.530	0.533	0.539
2.5	0.412	0.414	0.420
3.0	0.295	0.296	0.300
3.5	0.219	0.220	0.224
4.0	0.158	0.158	0.161
4.5	0.121	0.121	0.123
5.0	0.092	0.092	0.094

Meigooni and the Virtual Water used in this work were submitted to a chemical analysis laboratory (Analytical Answers Inc., Woburn, MA) for evaluation. The primary constituent in both samples was determined to be an epoxy resin with added calcium carbonate. The samples differed in the relative amount of calcium. By formulation, the materials should contain 2.3% calcium by mass (11). The amount in the Virtual Water sample was 2.4% calcium by mass, whereas the amount in the Solid Water sample was 1.7%. By using the mass attenuation coefficients for 20-keV photons (12), one can make a rough approximation of the expected effect the difference in the calcium content would make on the radial dose function determined in the two media. The average linear attenuation coefficient weighted by fractional mass for the elemental components yields 0.81 cm^{-1} for the sample of Virtual Water and 0.73 cm^{-1} for the Solid Water sample. This is assuming that the radial dose function would approximately follow the form $g(r) = Ae^{-\mu eff t}$, where A is the build-up factor. Because the radial dose function for r = 2 cm equals the dose at 2 cm divided by the dose at 1 cm (ignoring geometric attenuation), the approximate form yields $g(2\text{ cm}) = Ae^{-\mu eff \cdot 1\text{ cm}}$. The ratio of the radial dose functions at 2 cm for the two materials, R, becomes

$$R = g(2\text{cm})_{sw}/g(2\text{cm})_{vw} = Ae^{-(\mu_{eff}\cdot 1\text{cm})_{sw}}/Ae^{-(\mu_{eff}\cdot 1\text{cm})_{vw}} \quad (17)$$

The build-up factors cancel, leaving the ratio of the exponentials and R = 1.08. Multiplying the ratio by our value for the radial dose function at 2 cm, $g(2\text{ cm})$ = 0.53, the projected value for the radial dose function at 2 cm in the Solid Water phantom is 0.57. This agrees with the value reported by Meigooni to within 3%. This rough approximation makes many assumptions that likely fall within the desired uncertainties. However, the relatively close agreement between the rough calculation and the measured difference supports the hypothesis that the difference in the calcium content in the two phantoms could account for the slightly different results. Other factors for this difference could also

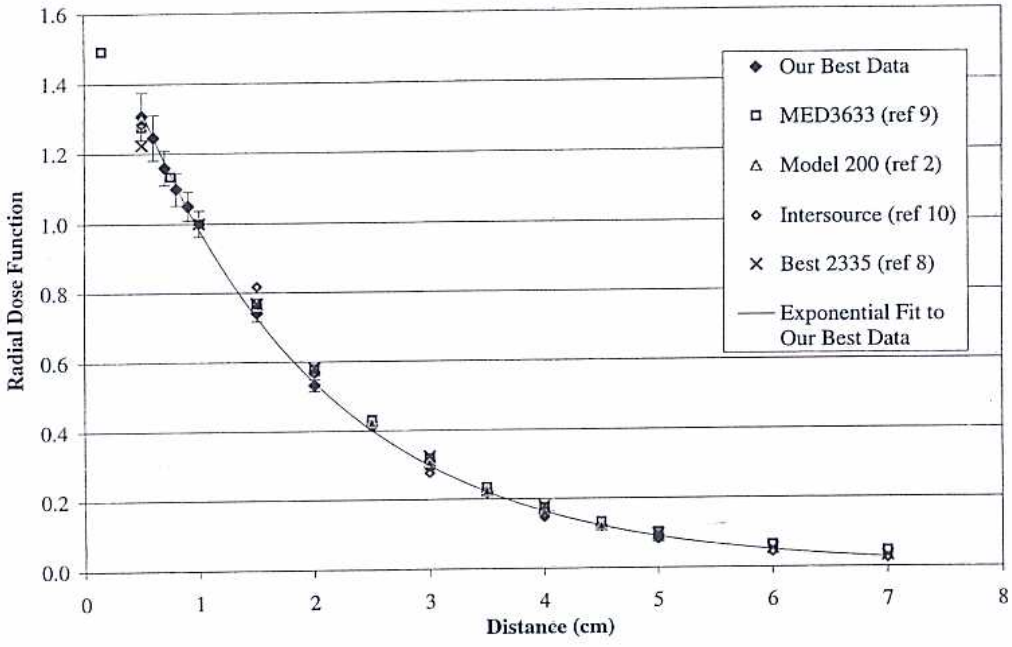

Fig. 3. The graph of the line source model radial dose function compared with other ^{103}Pd sources.

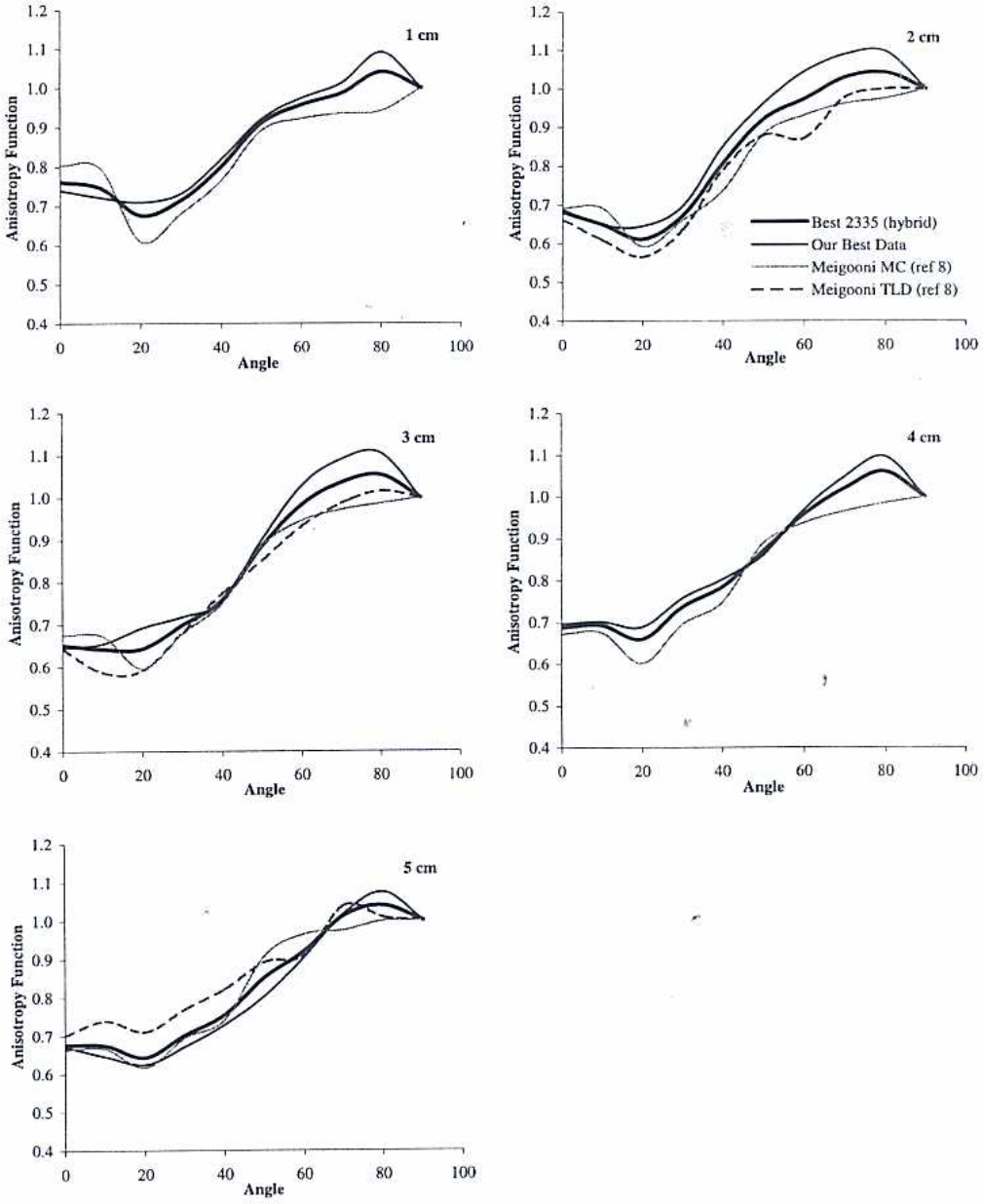

Fig. 4. Comparison of anisotropy functions, $F(r,\theta)$, for ^{103}Pd at given distances as determined in this work, that of Meigooni *et al.* (*8*), and the hybrid function. MC = Monte Carlo; TLD = thermoluminescent dosimeter.

be the phantom construction and the geometry factors used. It is assumed that Meigooni used the line source model. Because the calcium content of the Virtual Water phantom agreed with the accepted formulation and the values presented by Meigooni agree when corrected for the calcium content, it is suggested that the radial dose function from this work be used clinically.

Anisotropy function comparison

Figure 4 compares the current anisotropy data, calculated with the line source model geometry factors, with the measurements taken by Meigooni. The difference in calcium content of the phantom materials would make no difference in the anisotropy calculations for the ratio of measured values performed at the same distance. The hybrid used an average of our measurements and Meigooni's. However, Meigooni presented both TLD measurements and Monte Carlo (MC) simulation values; the MC values were provided at all distances, whereas the TLD measurements were performed only at 2, 3, and 5 cm. At these distances, with the data of Meigooni, both MC and TLD data were averaged, and that value was averaged with the measurements in this work. At the other distances—1 and 4 cm—the MC data of Meigooni were combined with the TLD data from this article at the ra-

Table 5
Measured values for the anisotropy function and the anisotropy factors for the Best ^{103} Pd radioactive source

	θ (°)										Anisotropy
r (cm)	0	10	20	30	40	50	60	70	80	90	factors
0.5	0.80	0.78	0.77	0.78	0.85	0.94	0.94	0.95	0.95	1.00	0.98
0.6	0.85	0.79	0.77	0.80	0.86	0.92	0.94	0.96	0.98	1.00	0.96
0.7	0.87	0.79	0.76	0.82	0.85	0.90	0.93	0.96	1.01	1.00	0.96
0.8	0.82	0.77	0.74	0.79	0.84	0.89	0.93	0.97	1.04	1.00	0.94
0.9	0.77	0.74	0.73	0.76	0.83	0.90	0.95	1.00	1.07	1.00	0.95
1.0	0.74	0.72	0.71	0.73	0.82	0.92	0.97	1.01	1.09	1.00	0.96
1.5	0.70	0.66	0.63	0.70	0.83	0.99	1.04	1.07	1.10	1.00	0.94
2.0	0.69	0.65	0.64	0.70	0.85	0.96	1.04	1.09	1.10	1.00	0.98
2.5	0.67	0.64	0.68	0.71	0.77	0.90	1.01	1.08	1.10	1.00	0.92
3.0	0.64	0.66	0.69	0.72	0.75	0.90	1.03	1.09	1.11	1.00	0.95
3.5	0.66	0.68	0.70	0.73	0.79	0.88	1.01	1.09	1.13	1.00	0.95
4.0	0.70	0.70	0.69	0.76	0.80	0.86	0.97	1.05	1.10	1.00	0.93
4.5	0.71	0.68	0.68	0.74	0.79	0.81	0.91	1.01	1.08	1.00	0.89
5.0	0.67	0.65	0.62	0.67	0.73	0.80	0.91	1.02	1.07	1.00	0.88

tio of one-third to two-thirds, respectively. The averaging was performed across both angle and distance. Figure 5 compares this hybrid anisotropy with that of other ^{103}Pd sources. The hybrid anisotropy function values are listed in Table 7.

Anisotropy constant comparison

Table 3 shows the anisotropy constant measured in this work and compares it with other ^{103}Pd sources. Calculation of the anisotropy constant, as discussed in TG-43, is vague, and the formula to use is not clear. TG-43 describes an equation for the anisotropy factors, but not for the anisotropy constant. This article considers three possible methods for calculating the anisotropy constant from the anisotropy factors, shown in Table 3. The first is taking the average of the anisotropy factors. The second is taking the sum of the anisotropy factors weighted by the radial dose function. The third is also a summation, but weighted with the radial dose function and a geometry factor, $1/r^2$. The two summation methods yield results indistinguishable within the uncertainty of the measurements. The inclusion of the geometry factor renders minimal contribution from the distances greater than 1 cm to the value of the anisotropy constant. The method used to calculate the anisotropy constant for the other ^{103}Pd sources in Table 3 was not always clear.

Conclusion

The measurements mentioned previously were to help establish the dosimetric constants for the new Best ^{103}Pd source. Values suggested for the clinical applications are 0.70 $cGy \cdot h^{-1} \cdot U^{-1}$ for the dose rate constant, 0.92 for the anisotropy constant, the geometry factor for the line source, the radial dose function in Table 4 for a line source, and the anisotropy functions and factors in Table 7.

Table 6
Geometry factor comparisons

	θ(°)									
r (cm)	0	10	20	30	40	50	60	70	80	90
0.5	5.96%	5.70%	4.97%	3.84%	2.48%	1.07%	−0.22%	−1.25%	−1.91%	−2.13%
0.6	4.27%	4.09%	3.57%	2.77%	1.82%	0.81%	−0.11%	−0.85%	−1.33%	−1.49%
0.7	3.19%	3.06%	2.67%	2.09%	1.38%	0.63%	−0.06%	−0.62%	−0.98%	−1.10%
0.8	2.47%	2.37%	2.07%	1.62%	1.07%	0.50%	−0.04%	−0.47%	−0.75%	−0.84%
0.9	1.97%	1.88%	1.65%	1.29%	0.86%	0.40%	−0.02%	−0.37%	−0.59%	−0.67%
1.0	1.60%	1.53%	1.35%	1.06%	0.70%	0.33%	−0.01%	−0.30%	−0.48%	−0.54%
1.5	0.72%	0.69%	0.61%	0.48%	0.32%	0.15%	0.00%	−.13%	−0.21%	−0.24%
2.0	0.41%	0.39%	0.34%	0.27%	0.18%	0.09%	0.00%	−0.07%	−0.12%	−0.14%

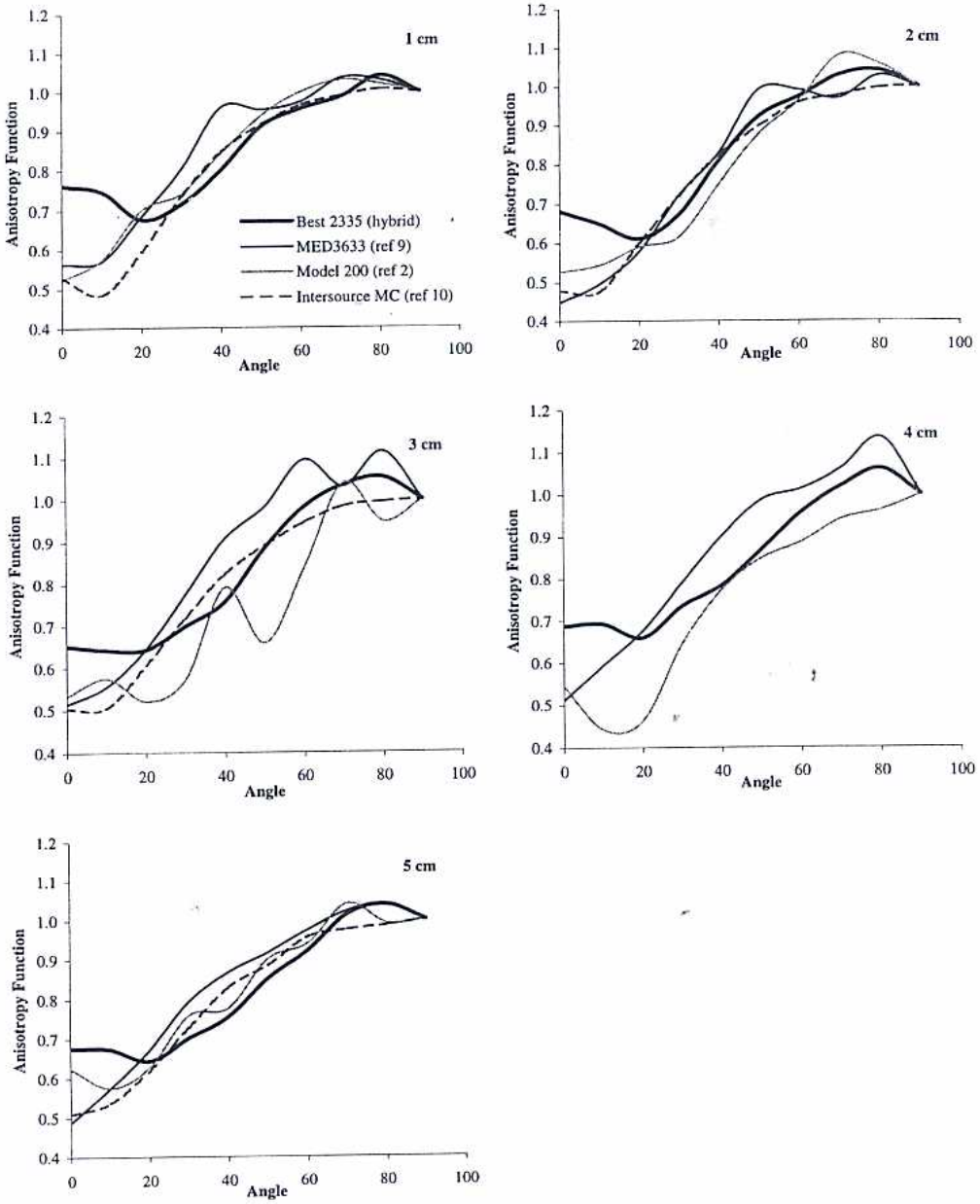

Fig. 5. Comparison of the hybrid anisotropy function to that for other ^{103}Pd sources. MC = Monte Carlo.

Acknowledgments

We thank the following supporters of this work: Best Medical International for supplying the sources; MED-CAL, Inc., for providing the blocks of Virtual Water; Bicron Corp. for providing the TLDs; and the University of Wisconsin Accredited Dosimetry Calibration Laboratory for calibrating the sources and the TLDs and reading the dosimeters.

Table 7
Calculated values for the anisotropy function based on the combination of our measured data and Meigooni's data for the Best Model 2335 ^{103}Pd seed

	Anisotropy function, θ (°)										Anisotropy
r (cm)	0	10	20	30	40	50	60	70	80	90	factor
1.0	0.74	0.72	0.68	0.71	0.80	0.91	0.96	0.99	1.04	1.00	0.93
2.0	0.68	0.65	0.61	0.67	0.81	0.92	0.97	1.03	1.04	1.00	0.92
3.0	0.65	0.64	0.64	0.70	0.76	0.88	0.98	1.03	1.05	1.00	0.91
4.0	0.69	0.69	0.66	0.74	0.78	0.87	0.96	1.02	1.06	1.00	0.91
5.0	0.68	0.67	0.64	0.70	0.75	0.85	0.92	1.01	1.04	1.00	0.89

References

[1] Williamson JF, Coursey BM, DeWerd LA, *et al*. Dosimetric prerequisites for routine clinical use of new low energy photon interstitial brachytherapy sources. *Med Phys* 1998;25:2269–2270.

[2] Nath R, Anderson LL, Luxton G, *et al*. Dosimetry of interstitial brachytherapy sources: Recommendations of the AAPM Radiation Therapy Committee Task Group No. 43. *Med Phys* 1995;22:209–234.

[3] Van Grieken RE, Markowicz AJ, eds. Handbook of X-ray spectrometry: methods and techniques. 2nd ed. New York: Marcel Dekker; 1993.

[4] Hartmann GH, Schlegel W, Scharfenberg H. The three-dimensional dose distribution of ^{125}I seeds in tissue. *Phys Med Biol* 1983;28:693–699.

[5] Weaver KA. Response of LiF powder to ^{125}I photons. *Med Phys* 1984;11:850–854.

[6] Meigooni AS, Meli JA, Nath R. A comparison of solid phantoms with water for dosimetry of ^{125}I brachytherapy sources. *Med Phys* 1988;15:695–701.

[7] Furhang EE, Wallace RE. Fitting and benchmarking of dosimetry data for new brachytherapy sources. *Med Phys* 2000;27:2302–2306.

[8] Meigooni AS, Bharucha Z, Yoe-Sein M, *et al*. Dosimetric characteristics of the Best® double-wall ^{103}Pd brachytherapy source. *Med Phys* 2001;28:2568–2575.

[9] Wallace RE, Fan JJ. Dosimetric characterization of a new design ^{103}palladium brachytherapy source. *Med Phys* 1999;26:2465–2470.

[10] Meigooni AS, Sowards K, Soldano M. Dosimetric characteristics of the Intersource ^{103}palladium brachytherapy source. *Med Phys* 2000; 27:1093–1100.

[11] Constantinou C, Attix FH, Paliwal BR. A solid water phantom material for radiotherapy x-ray and γ-ray beam calibrations. *Med Phys* 1982;9:436–441.

[12] Hubbell JH. Photon mass attenuation and energy-absorption coefficients from 1 keV to 20 MeV. *Int J Appl Radiat Isot* 1982;33: 1269–1290.